Stem Cell Reports, Volume *17*

Supplemental Information

A human pluripotent stem cell-based model of SARS-CoV-2 infection reveals an ACE2-independent inflammatory activation of vascular endothelial cells through TLR4

Zhangjing Ma, Xisheng Li, Rebecca L.Y. Fan, Kevin Y. Yang, Calvin S.H. Ng, Rainbow W.H. Lau, Randolph H.L. Wong, Kevin K. Ng, Chi Chiu Wang, Peng Ye, Zelong Fu, Alex W.H. Chin, M.Y. Alison Lai, Yu Huang, Xiao Yu Tian, Leo L.M. Poon, and Kathy O. Lui

Supplemental Figures and Legends

Figure S1 Validation of the anti-ACE2 antibody. Western blotting showing ACE2 expression using 0.5 ug human recombinant ACE2 protein.

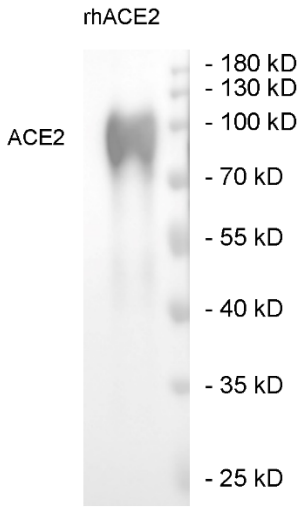

Figure S2 SARS-CoV-2 does not influence EC survival. Immunostaining for cleaved caspase-3 (cCASP3) on ACE2-deficient and -expressing hESC-ECs at (F) 48 and (G) 72 hours after inoculation with SARS-CoV-2 (virus) or culture medium (mock infection controls), respectively. Scale bars: 200 μm.

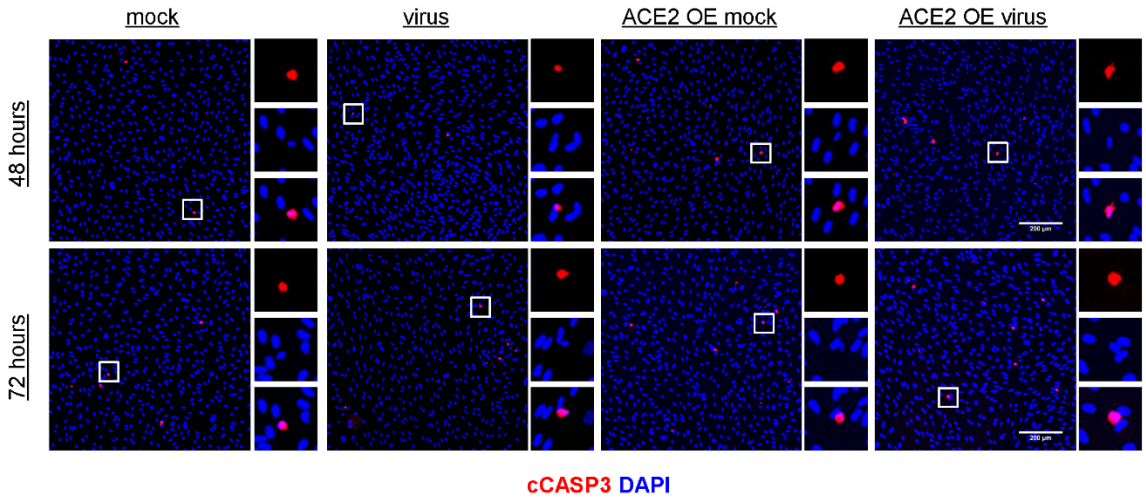

Figure S3 GO enrichment analyses showing a list of upregulated and downregulated pathways in 17 clusters of circulating ECs of COVID-19 patients. A total of 2,236 $CD31^{+}CD45^{-}$ circulating ECs out of 139,848 PBMCs collected from 50 samples containing 8 mild, 9 severe COVID-19 patients and 13 controls recruited in the same cohort of a previous study (Schulte-Schrepping *et al*., 2020). A selection of top 3 pathways in terms of biological processes of each cluster determined by Gene Ontology (GO) associated to genes detected as significantly upregulated and downregulated ($P<0.05$), respectively, in scRNA-seq comparing expression of that gene to the rest of the clusters, differences were determined by Seurat's implementation of the Wilcoxon rank-sum test. Related to Table S1 (upregulated pathways) and Table S2 (downregulated pathways).

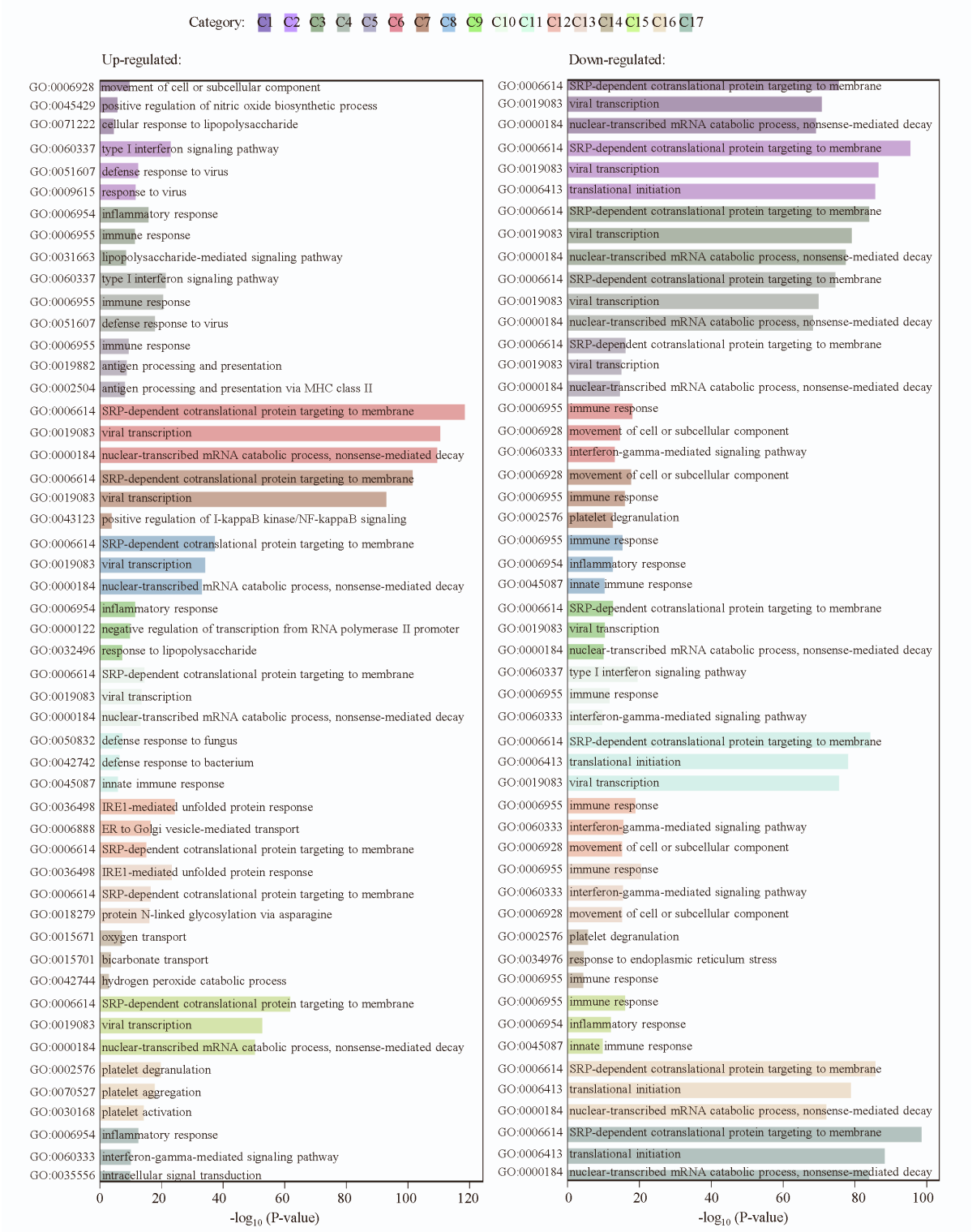
Category: C1 C2 C3 C4 C5 C6 C7 C8 C9 C10 C11 C12 C13 C14 C15 C16 C17
Up-regulated:
GO:0006928 movement of cell or subcellular component
GO:0045429 positive regulation of nitric oxide biosynthetic process
GO:0071222 cellular response to lipopolysaccharide
GO:0060337 type I interferon signaling pathway
GO:0051607 defense response to virus
GO:0009615 response to virus
GO:0006954 inflammatory response
GO:0006955 immune response
GO:0031663 lipopolysaccharide-mediated signaling pathway
GO:0060337 type I interferon signaling pathway
GO:0006955 immune response
GO:0051607 defense response to virus
GO:0006955 immune response
GO:0019882 antigen processing and presentation
GO:0002504 antigen processing and presentation via MHC class II
GO:0006614 SRP-dependent cotranslational protein targeting to membrane
GO:0019083 viral transcription
GO:0000184 nuclear-transcribed mRNA catabolic process, nonsense-mediated decay
GO:0006614 SRP-dependent cotranslational protein targeting to membrane
GO:0019083 viral transcription
GO:0043123 positive regulation of I-kappaB kinase/NF-kappaB signaling
GO:0006614 SRP-dependent cotranslational protein targeting to membrane
GO:0019083 viral transcription
GO:0000184 nuclear-transcribed mRNA catabolic process, nonsense-mediated decay
GO:0006954 inflammatory response
GO:0000122 negative regulation of transcription from RNA polymerase II promoter
GO:0032496 response to lipopolysaccharide
GO:0006614 SRP-dependent cotranslational protein targeting to membrane
GO:0019083 viral transcription
GO:0000184 nuclear-transcribed mRNA catabolic process, nonsense-mediated decay
GO:0050832 defense response to fungus
GO:0042742 defense response to bacterium
GO:0045087 innate immune response
GO:0036498 IRE1-mediated unfolded protein response
GO:0006888 ER to Golgi vesicle-mediated transport
GO:0006614 SRP-dependent cotranslational protein targeting to membrane
GO:0036498 IRE1-mediated unfolded protein response
GO:0006614 SRP-dependent cotranslational protein targeting to membrane
GO:0018279 protein N-linked glycosylation via asparagine
GO:0015671 oxygen transport
GO:0015701 bicarbonate transport
GO:0042744 hydrogen peroxide catabolic process
GO:0006614 SRP-dependent cotranslational protein targeting to membrane
GO:0019083 viral transcription
GO:0000184 nuclear-transcribed mRNA catabolic process, nonsense-mediated decay
GO:0002576 platelet degranulation
GO:0070527 platelet aggregation
GO:0030168 platelet activation
GO:0006954 inflammatory response
GO:0060333 interferon-gamma-mediated signaling pathway
GO:0035556 intracellular signal transduction
0 20 40 60 80 100 120
-log10 (P-value)
Down-regulated:
GO:0006614 SRP-dependent cotranslational protein targeting to membrane
GO:0019083 viral transcription
GO:0000184 nuclear-transcribed mRNA catabolic process, nonsense-mediated decay
GO:0006614 SRP-dependent cotranslational protein targeting to membrane
GO:0019083 viral transcription
GO:0006413 translational initiation
GO:0006614 SRP-dependent cotranslational protein targeting to membrane
GO:0019083 viral transcription
GO:0000184 nuclear-transcribed mRNA catabolic process, nonsense-mediated decay
GO:0006614 SRP-dependent cotranslational protein targeting to membrane
GO:0019083 viral transcription
GO:0000184 nuclear-transcribed mRNA catabolic process, nonsense-mediated decay
GO:0006614 SRP-dependent cotranslational protein targeting to membrane
GO:0019083 viral transcription
GO:0000184 nuclear-transcribed mRNA catabolic process, nonsense-mediated decay
GO:0006955 immune response
GO:0006928 movement of cell or subcellular component
GO:0060333 interferon-gamma-mediated signaling pathway
GO:0006928 movement of cell or subcellular component
GO:0006955 immune response
GO:0002576 platelet degranulation
GO:0006955 immune response
GO:0006954 inflammatory response
GO:0045087 innate immune response
GO:0006614 SRP-dependent cotranslational protein targeting to membrane
GO:0019083 viral transcription
GO:0000184 nuclear-transcribed mRNA catabolic process, nonsense-mediated decay
GO:0060337 type I interferon signaling pathway
GO:0006955 immune response
GO:0060333 interferon-gamma-mediated signaling pathway
GO:0006614 SRP-dependent cotranslational protein targeting to membrane
GO:0006413 translational initiation
GO:0019083 viral transcription
GO:0006955 immune response
GO:0060333 interferon-gamma-mediated signaling pathway
GO:0006928 movement of cell or subcellular component
GO:0006955 immune response
GO:0060333 interferon-gamma-mediated signaling pathway
GO:0006928 movement of cell or subcellular component
GO:0002576 platelet degranulation
GO:0034976 response to endoplasmic reticulum stress
GO:0006955 immune response
GO:0006955 immune response
GO:0006954 inflammatory response
GO:0045087 innate immune response
GO:0006614 SRP-dependent cotranslational protein targeting to membrane
GO:0006413 translational initiation
GO:0000184 nuclear-transcribed mRNA catabolic process, nonsense-mediated decay
GO:0006614 SRP-dependent cotranslational protein targeting to membrane
GO:0006413 translational initiation
GO:0000184 nuclear-transcribed mRNA catabolic process, nonsense-mediated decay
0 20 40 60 80 100
-log10 (P-value)

Supplemental Tables

Table S1 Patient information in this study. *The age of adult samples is indicated in years old while that of fetal samples is indicated as zero as they were collected immediately after birth.

Tissue type	**Sex**	**Age***	**Diagnosis**
Aorta	M	56	Aortic dissection
	F	60	Aortic dissection
	F	68	Aortic dissection
	F	71	Aortic dissection
	M	72	Thoracic aortic aneurysm
Lung	F	38	Right upper lobe adenocarcinoma of lung
	F	53	Left upper lobe adenocarcinoma of lung
	M	58	Left upper lobe adenocarcinoma of lung
	F	58	Right lower lobe adenocarcinoma of lung
	F	64	Right lower lobe adenocarcinoma of lung
	M	66	Right lower lobe adenocarcinoma of lung
	M	68	Left upper lobe adenocarcinoma of lung
	F	68	Right lower lobe adenocarcinoma of lung
	F	70	Left upper lobe adenocarcinoma of lung
	M	71	Left upper lobe adenocarcinoma of lung
	M	71	Right upper lobe adenocarcinoma of lung
	M	73	Left upper lobe adenocarcinoma of lung
	F	75	Right upper lobe adenocarcinoma of lung
	F	78	Left lower lobe adenocarcinoma of lung
	F	80	Right lower lobe adenocarcinoma of lung
Liver	M	53	Hepatocellular carcinoma
	M	58	Hepatocellular carcinoma
	M	60	Hepatocellular carcinoma
	M	66	Hepatocellular carcinoma
	M	67	Hepatocellular carcinoma
Umbilical cord	F	0	Healthy

	M	0	Healthy
	M	0	Healthy
	M	0	Healthy
	F	0	Healthy
Placenta	F	0	Healthy
	M	0	Healthy
	M	0	Healthy
	M	0	Healthy
	F	0	Healthy

Table S2 GO enrichment analyses showing a list of upregulated genes expressed in 17 clusters of circulating ECs of COVID-19 patients. A total of 2,236 $CD31^{+}CD45^{-}$ circulating ECs out of 139,848 PBMCs collected from 50 samples containing 8 mild, 9 severe COVID-19 patients and 13 controls recruited in the same cohort of a previous study (Schulte-Schrepping *et al*., 2020). A selection of top 3 pathways in terms of biological processes of each cluster determined by Gene Ontology (GO) associated to genes detected as significantly upregulated ($P<0.05$) in scRNA-seq comparing expression of that gene to the rest of the clusters, differences were determined by Seurat's implementation of the Wilcoxon rank-sum test. Related to Figure 6G and H.

(see Table S2.xlsx)

Table S3 GO enrichment analyses showing a list of downregulated genes expressed in 17 clusters of circulating ECs of COVID-19 patients. A total of 2,236 $CD31^{+}CD45^{-}$ circulating ECs out of 139,848 PBMCs collected from 50 samples containing 8 mild, 9 severe COVID-19 patients and 13 controls recruited in the same cohort of a previous study (Schulte-Schrepping *et al*., 2020). A selection of top 3 pathways in terms of biological processes of each cluster determined by Gene Ontology (GO) associated to genes detected as significantly downregulated ($P<0.05$) in scRNA-seq comparing expression of that gene to the rest of the clusters, differences were determined by Seurat's implementation of the Wilcoxon rank-sum test. Related to Figure 6G and H.

(see Table S3.xlsx)

Supplemental Experimental Procedures

Cell cultures

All cells were cultured in a humidified 5% CO_2 37ºC tissue culture incubator. Cell type-specific culture conditions are listed below.

Human ECs

The experimental human EC lines HUVEC (Lonza, Cat No. C2517A) and HMVEC-L (Lonza, Cat No. CC-2527) were maintained in EGM-2 BulletKit™ (Lonza) supplemented with 10% and 20% FBS, respectively.

hESC

The H9 hESC line (WiCell, WA09) was maintained in mTesR1 medium (StemCell Technologies).

hESC-EC differentiation

hESC-ECs were differentiated from hESCs under defined conditions as previously described (Leung *et al.*, 2019; Lui *et al.*, 2014; Lui *et al.*, 2013). Briefly, hESC were cultured in mesoderm differentiation medium containing 50% DMEM/F12-Glutamax and 50% neurobasal media supplemented with 1% N2, 2% B27, 50 μM 2-mercaptoethanol and 2 mM L-glutamine (Gibco). Growth factors and small molecules including 25 ng/ml BMP4 (Peprotech, Cat No. AF-120-05ET) and 8 μM CHIR99021 (Selleck Chem, Cat No. S2924) were added to the mesoderm differentiation medium from day 1 to day 4. From day 4 onwards, hESC were cultured in EC differentiation medium containing StemPro medium (Gibco) supplemented with 200 ng/ml VEGF-A (Perprotech, Cat No. 100-20) and 2 μM forsokolin (Abcam, Cat No. ab120058). At day 6, differentiated $CD31^+CD144^+$ hESC-ECs were dissociated by TrypLE Express (Thermo Fisher Scientific), purified by magnetic-associated cell sorting using CD144 Microbeads (Miltenyi Biotec, Cat No. 130-097-857) and maintained in EGM-2 medium. In some experiments, hESC-ECs were treated with the following recombinant proteins or small molecules including 10-100 ng/ml IL-1β (Peprotech, Cat No. 200-01B), IL-6 (Peprotech, Cat No. 200-06), TNF-α (Peprotech, Cat No. 300-01A) or IFN-γ (Peprotech, Cat No. 300-02); 1 μM CLI095 (Invivogen, Cat No. Tlrl-cli95); or 10 μM dexamethasone (Sigma, Cat No. D1756).

Human monocytes

The human monocyte cell line THP-1 (ATCC, TIB-202) was maintained in RPMI-1640 supplemented with 10% FBS, 50 μM 2-mercaptoethanol, penicillin and streptomycin.

African green monkey Vero E6 cells

The renal epithelial cell line Vero E6 (ATCC, CRL-1586) was maintained in DMEM supplemented with 10% FBS, penicillin and streptomycin.

SARS-CoV-2 quantification

At 24, 48 and 72 hours after infection at 37°C, viral quantification was performed using two assays, RT-qPCR for viral RNA (vRNA) and the $TCID_{50}$ assay for determining the infectious viral titers. For RT-qPCR, 140μl supernatant of the indicated types of human EC cultures was collected and vRNA was extracted using the QIAamp Viral RNA Mini Kit (Qiagen). vRNA was quantified using the N gene RT-qPCR assay as previously described (Chu *et al*., 2020). For $TCID_{50}$, SARS-CoV-2-containing supernatant of ACE2-deficient or -expressing hESC-ECs was added to confluent Vero E6 cells, and the cytopathic effect was read at day 4 post infection.

Lentiviral vector-mediated ACE2 overexpression

hESC-ECs were transduced with lentiviral vectors containing ACE2 (Vigene Biosciences) at MOI of 20 in prewarmed culture medium supplemented with 8 ug/ml polybrene (Sigma) for 24 hours at 37°C. On the next day, transduction medium was replaced by culture medium. Surface ACE2 expression was detected by flow cytometry and total ACE2 was assessed by western blotting at day 3 after transduction.

Flow cytometry

Human tissues were minced into small fragments and dissociated in 50% F-10 medium (Sigma) and 50% PBS supplemented with 500 U/ml type II collagenase (Worthington) and 5.5 U/ml dispase (Gibco) at 37°C for 30 minutes. Enzymatic reactions were diluted by adding 10% FBS and the dissociated cells were washed twice with PBS. The dissociated cells were removed from the contaminated erythrocytes by incubating in red blood cell lysis buffer (eBiosciences) for 5 minutes.

Single cells derived from human tissues or hESC-ECs were blocked with 2% FBS followed by staining with fluorescence conjugated antibodies targeting ACE2 (R&D Systems, FAB933G), CD31 (Biolegend, 303106), CD45 (eBioscience, 17-0459-42), CD144 (R&D Systems, FAB9381A) or isotype controls for 30 minutes on ice. Cells were then washed thrice with FACS buffer and DAPI (BD Biosciences) positive dead cells were excluded for live cell analysis. Fluorescence labelled single cells were then processed on flow cytometer (Beckman Coutler CytoFLEX) and FACS data were further analyzed with the FlowJo software (Tree star).

Vascular permeability assay

ACE2-deficient or -expressing hESC-ECs and HUVEC were seeded on collagen-coated transwell filters (8-μm pore size, SPL) in the upper chamber of a 24-well dish and allowed to grow until confluent at 37°C. Cells were preincubated with SARS-CoV-2 (0.1 MOI) or culture medium (mock infection controls) for 1 hour. Infection medium in the upper chamber and lower compartment was then replaced by culture medium. At 72 hours after viral inoculation, 70 kDa fluorescein isothiocyanate (FITC)-dextran (Sigma, FD70S) at a final concentration of 0.5 mg/ml was added to the upper chamber. After 30 minutes, the FITC-dextran containing medium at the lower compartment was supplemented with paraformaldehyde (PFA) at a final concentration of 4% for 1 hour to inactivate the virus. The fluorescent content in each sample was measured at an excitation wavelength of 485 nm and an emission wavelength of 530 nm using a fluorescence plate reader (PerkinElmer Victor^{TM} X4).

Monocyte adhesion assay

THP-1 cells were labelled with CellTrace^{TM} Yellow Cell Proliferation Kit (Thermofisher Scientific, C34567) for 30 minutes at 37°C and then washed thrice in culture medium before counting. Before adhesion experiments, ACE2-deficient or -expressing hESC-ECs and HUVEC on the chamber slides were treated with culture medium (mock infection controls) or SARS-CoV-2 (0.1 MOI) for 1 hour at 37°C. Infection medium was then replaced by culture medium. In some experiments, human ECs were also treated with CLI095 or dexamethasone. At 72 hours following viral inoculation, 10^6/ml THP-1 were deposited on hESC-ECs for 1 hour at 37°C. Wells were then washed extensively to eliminate nonadherent cells, and then adherent cells were fixed with 4% PFA for 1 hour before counterstained with DAPI. The degree of monocyte adhesion was quantified

by blind count per unit area using this formula: THP-1/hESC-ECs or /HUVEC.

Assessment of NO production

ACE2-deficient hESC-ECs and HUVEC were preincubated with culture medium (mock infection controls) or SARS-CoV-2 (0.1 MOI) for 1 hour at 37°C. Infection medium was then replaced by culture medium. In some experiments, human ECs were also treated with CLI095 or dexamethasone. At 72 hours after viral inoculation, cells were supplemented with the NO probe, DAF-FM diacetate (ThermoFisher, Cat. No., D23844, 10 μmol/L, 60 min, 37 °C) in culture medium at pH 7.4. Excessive probe was removed by washing cells with PBS followed by incubation in fresh medium for an additional 30 min to allow complete de-esterification of the intracellular diacetate. After that, cells were harvested and fixed with 4% PFA for 1 hour followed by washing and resuspension in PBS. Fluorescent signal was taken at 495 nm excitation and 515 nm emission at room temperature.

Immunostaining

ACE2-deficient or -expressing hESC-ECs were preincubated with culture medium (mock) or SARS-CoV-2 (0.1 MOI) for 1 hour at 37°C. Infection medium was then replaced by culture medium. At 48 or 72 hours after inoculation at 37°C, hESC-ECs were fixed in 4% paraformaldehyde at room temperature for 1 hour. The fixed cells were washed thrice with PBS and blocked with 10% donkey serum followed by staining with the anti-cCASP3 (Cell Signaling Technology, 9661L) antibody at 4°C overnight. Alexa-Fluor-594 conjugated secondary antibody (Invitrogen) was used at room temperature for 30 min in the dark. Slides were mounted with DAPI-containing fluorescence mounting medium (Thermo Fisher), and fluorescence was detected with a fluorescence microscope (Leica). Cell viability was quantified by blind count per unit area using this formula: $cCASP3^+$ cells / hESC-ECs x 100%.

Western Blotting

Human lung tissues were minced into small fragments and dissociated in 50% F-10 medium (Sigma) and 50% PBS supplemented with 500 U/ml type II collagenase (Worthington) and 5.5 U/ml dispase (Gibco) at 37°C for 30 minutes. Enzymatic reactions were diluted by adding 10% FBS and the dissociated cells were washed twice with PBS. The dissociated cells were removed from the contaminated erythrocytes by incubating in red blood cell lysis buffer (eBiosciences) for

5 minutes. Single cells were further processed for EC and non-EC isolation using the human CD31 MicroBead Kit (Miltenyi Biotec, Cat. No. 130-091-935) per manufacturer's instruction before protein extraction. hESC-ECs from cell cultures were isolated as follows. ACE2-deficient or -expressing hESC-ECs were preincubated with culture medium (mock) or SARS-CoV-2 (0.1 MOI) for 1 hour at 37°C. Infection medium was then replaced by culture medium. In some experiments, HUVEC was also treated with CLI095 or dexamethasone. At 48 or 72 hours after inoculation, ACE2-deficient or -expressing hESC-ECs and HUVEC derived from different treatment groups were harvested. Protein was extracted from these cells by pipetting up-and-down in radioimmunoprecipitation assay (RIPA) buffer (Beyotime) supplemented with protease and phosphatase inhibitors (Roche) for 30 minutes at 4°C. After that, the mixture was boiled in SDS loading buffer at 95°C for 10 minutes. 10-15 micrograms of protein was used for each experiment. In antibody specificity assessment, 0.5 micrograms of recombinant human ACE2 (Biolegend, Cat No. 792002) was used. The following dilutions of each antibody were used: ACE2 (R&D systems, AF933, 1:1000), p38 MAPK (Cell Signaling Technology/CST, 8690, 1:1000), p-p38 MAPK at Thr180/Tyr182 (CST, 9211, 1:1000), NF_KB p65 (CST, 8242, 1:1000), p-NF_KB p65 at Ser536 (CST, 3033, 1:1000), IL-1β (CST, 12242, 1:1000), e-NOS (BD Biosciences, Cat. No. 610297, 1:1000), p-eNOS at Ser632 (abcam, Cat. No. ab76199, 1:500), and β-actin (ImmunoWay, YM3028, 1:7000). The relative band intensities were quantified using the ImageJ software; and the relative protein expression level of each sample was compared with an internal control such as mock control.

Real time qPCR

Total RNA was isolated using RNeasy mini kit (Qiagen) and reverse transcribed using iScript cDNA synthesis kit (Bio-Rad), according to manufacturers' instructions. RT-qPCR was analysed on QuantStudio^{TM} 12K Flex Read-Time PCR system (ThermoFisher Scientific) via SYBR Green (Bio-Rad). Values for specific genes were normalized to the housekeeping controls, *GAPDH*. The relative gene expression level of each sample was also compared with an internal control such as mock controls. The primer sequences used are as follows:

ACE2: forward – 5'TCCATTGGTCTTCTGTCACCCG3'

ACE2: reverse – 5'AGACCATCCACCTCCACTTCTC3'

IL-1β: forward - 5'CCACAGACCTTCCAGGAGAATG3'

IL-1β: reverse - 5'GTGCAGTTCAGTGATCGTACAGG3'

GAPDH: forward – 5' GTCTCCTCTGACTTCAACAGCG3'

GAPDH: reverse – 5' ACCACCCTGTTGCTGTAGCCAA3'

Supplemental References

Chu, D.K.W., Pan, Y., Cheng, S.M.S., Hui, K.P.Y., Krishnan, P., Liu, Y., Ng, D.Y.M., Wan, C.K.C., Yang, P., Wang, Q., et al. (2020). Molecular Diagnosis of a Novel Coronavirus (2019-nCoV) Causing an Outbreak of Pneumonia. Clin Chem *66*, 549-555. 10.1093/clinchem/hvaa029.

Leung, C. S., Li, J., Xu, F., Wong, A. S. L. & Lui, K. O. Ectopic expression of recipient CD47 inhibits mouse macrophage-mediated immune rejection against human stem cell transplants. *FASEB J* **33**, 484-493, doi:10.1096/fj.201800449R (2019).